Investigation of 3D water transport paths in gas diffusion layers by combined in-situ synchrotron X-ray radiography and tomography

H. Markötter [1]*, I. Manke [1], Ph. Krüger [2], T. Arlt [1], J. Haussmann [2], M. Klages [2], H. Riesemeier [3], Ch. Hartnig [4], J. Scholta [2], J. Banhart [1]

[1] Helmholtz Zentrum Berlin (HZB), Hahn-Meitner-Platz 1, 14109 Berlin, Germany

[2] Centre for Solar Energy and Hydrogen Research (ZSW), Helmholtzstraße 8, 89081 Ulm, Germany

[3] Federal Institute for Materials Research and Testing (BAM), Unter den Eichen 87, 12205 Berlin, Germany

[4] Chemetall GmbH, Trakehnerstr. 3, 60487 Frankfurt, Germany

*   Corresponding author:
E-mail address: henning.markoetter@helmholtz-berlin.de
Present address: Helmholtz Zentrum Berlin, Hahn-Meitner-Platz 1, 14109 Berlin, Germany
Tel.:   +49 30 8062 42826
Fax.:   +49 30 8062 43059

Abstract

The three-dimensional water distribution and water transport paths in the gas diffusion layer (GDL) and the adjacent micro-porous layer (MPL) of a polymer electrolyte membrane fuel cell (PEMFC) were analyzed during cell operation. The technique of quasi in-situ X-ray tomography was used for a 3D visualization of the water distribution and the structure of the GDL at different operating conditions. Based on findings from in-situ radiographic measurements water transport paths were detected and subsequently examined by tomography. The combination of these 2D and 3D techniques allows for a fully three-dimensionally resolved visualization of transport paths through the GDL.

Keywords (max. 6)

1. Introduction

One of the major tasks in the development of polymer electrolyte membrane fuel cells (PEMFCs) is the water management [1-4]. For good proton conductivity, the membrane requires a certain water content. A drying membrane loses some of its conductivity, which results in performance drops and the membrane might even undergo irreversible damage. On the other extreme, supply of the catalyst layer with reactant gases can be blocked by excess liquid water again accompanied by a detrimental impact on performance. The porous gas diffusion layer (GDL) is a key component that has to ensure optimal water management under a range of operating conditions. A goal-oriented development of GDL materials would benefit from a thorough insight into the three-dimensional water transport paths which is currently limited due to the lack of appropriate in-situ investigation techniques.

Neutron radiography is a well-established technique for non-destructive studies of water distribution during cell operation, but its spatial resolution is not sufficient to resolve individual small (10-50 µm) water agglomerates in the pores of a GDL [5-12]. In the recent years synchrotron X-ray radiography has been introduced for in-situ investigations of water in GDLs [13-16]. However the technique is limited to 2D projection imaging which does not reveal the structural details of the GDL that extend into the third dimension. On the other hand, X-ray tomography yields information about the 3D structure, but is not suited for fast in-situ measurements to analyze the dynamic water distribution [17, 18]. X-ray tomograms have been acquired in less than 1 s [19] but the X-ray intensity of the beams required in such experiments can damage the cell materials in use. Therefore, tomography with the beam appropriately adjusted, i.e. lower intensities, must be applied. In this approach, 2D in-situ measurements were employed to identify preferred paths for liquid water transport which were studied in more detail by quasi in-situ tomography.

2. Tomography setup

The presented work was carried out at the tomography station at the BAMline (Bessy II electron storage ring, Helmholtz-Zentrum Berlin, Germany) [20]. For tomographic

investigations, the fuel cell was mounted on a rotation table and rotated stepwise. 1800 radiographic projections at continuing rotation angles were taken over 180° and used for the tomographic reconstruction of the cell. A gadolinium oxysulphide (GadOx) scintillator screen was used to convert X-rays into visible light. A 4008×2672 pixel CCD detector (PCO4000) was used to detect the light. The field of view was about 19.2×12.8 mm² and the pixel size 4.8×4.8 μm². X-ray energies between 15 and 17 keV were chosen for the experiments.

3. Fuel cell setup

The PEM fuel cell investigated was specially designed and fabricated for the requirements of synchrotron X-ray tomography in terms of size and materials used. Its design ensures realistic conditions in terms of temperature and gas utilization. The anode and cathode flow fields were machined into plates of graphite as a meander-shaped single channel with a channel depth and width of 500 μm and ribs with the same width, see Fig. 1. A SGL 10 BC gas diffusion layer containing 5 wt.% PTFE and a micro-porous layer (MPL) were employed. A catalyst-coated membrane (CCM) composed of 50 μm thick Nafion 112 and platinum catalyst loading on both anode and cathode side was used. The cell was operated at a temperature of 50° C with stoichiometries of $\lambda_a = 2$ for the anode and of $\lambda_k = 2.5$ for the cathode. Current densities ranged from 40 to 160 mA/cm². In the area of view the metallic end plates were replaced by acrylic glass to allow for sufficient beam transmission. The horizontal cross section of the cell was a rectangular area of 13×14 mm².

4. Quasi in-situ tomography

The main problem of tomographic investigations is the long measuring time necessary to obtain a sufficient amount of projections (here 1800) which takes typically 20-100 min for this fuel cell. In order to prevent water movement during this time, fuel cell operation was stopped and the gas inlets and outlets were sealed before imaging. Except for some minor rearrangement of the fluids, the configuration inside the cell is preserved for tomography in this way. This 'quasi in-situ tomography' technique therefore reveals three-dimensional information on the GDL structure as well as the water distribution at

the time the cell was stopped. 2D in-situ radiographies were performed prior to tomography to investigate the water flow dynamics at current densities of 40 - 160 mA/cm².

5. Results

Figure 2 illustrates the evolution of water distribution in a selected cell section close to the turn of the flow field channels. The water distribution is quantified by normalizing every image with regard to a reference image taken earlier [13, 15] and, therefore, the images show water distribution changes with respect to the initial state. Newly formed water droplets appear bright and water that disappeared after the reference image was taken shows up dark (Fig. 2, channel boundaries). The change in water thickness can be read off the legend in Fig. 2a.

In the images in Fig. 2 one can see a mismatch of anode and cathode flow field channels (marked in Fig. 2b), so they do not overlap exactly in the through-plane images. In some cases this allows for position determination of observed water droplets relative to the channels. The images in Fig. 2a-f show the development of a droplet that forms in a straight segment of the cathode channel. It grows to a maximum volume of about 20 nanoliter within an overall time of 45 seconds. Then the droplet is rapidly dragged away by the streaming gas or by other water droplets that move fast through the channel. However, this event is too fast to be resolved temporally.

The location of the droplet was identified in the tomogram and closely examined. The slices of the tomogram displayed in Fig. 3c,d show a crack in the MPL located beneath a large GDL pore. It can be assumed that the crack and the pore are connected to form a direct transport path for water. According to Zhou et al. increased pore diameters result in reduced pressure gradients necessary to drive water through the GDL [21]. This means liquid water moving towards the flow field channels would be preferably transported via interconnected large GDL pores.

This assumption is further supported by tomographies which were taken subsequent to cell operation at different current densities. Figures 3e-j show slices along the y-z (Fig. 3e-g) and x-y planes (Fig. 3h-j) through the tomogram at the locations marked in Fig. 3c,d by yellow boxes. The three shown tomograms were taken at dry condition and

4

subsequent to cell operation at current densities of 80 and 160 mA/cm^2, respectively. At 80mA/cm^2 small water droplets are found in the MPL crack (Fig. 3f,i; red arrows). Even more water can be found at 160 mA/cm^2 (Fig. 3g,j; red arrows). Water droplets also accumulate in the GDL pores that form a possible transport pathway from the MPL crack into the flow field channel (Fig. 3j, black arrow). Most of the water feeding the analyzed droplet is expected to be produced in the area nearby and might take the transport path as indicated in Fig. 3h.

The findings indicate that the crack in the MPL and the wide pore build a preferred transport path into the flow field channel. Cracks provide an open spot where the initial water condensation might take place. This allows for a better water transport to the channel and might reduce the water saturation in the surrounding area which will improve the catalyst gas supply [22]. The 3D analysis might also contribute to the understanding of the performance increase found in studies of fuel cells with perforated GDLs [23]. Alink et. al. [24] explained this increase by an in-plane transport of liquid water towards the hole, that acts as drainage. Future analyses might focus on the investigation of the impact of the GDL structure (e.g. perforation) on the 3D water transport paths.

6. Conclusion

We presented a study of water transport paths in gas diffusion layers (GDL) of PEM fuel cells. By combining in-situ radiography with a quasi in-situ tomography technique, such transport paths could be revealed in an operating fuel cell in three dimensions for the first time. We found clear correlations between larger pores in the GDL and cracks in the micro-porous layer and could identify preferred water transport paths. The combination of radiography and tomography was demonstrated as a powerful method to characterize liquid water transport in GDL materials.

References

[1] W. Vielstich, A. Lamm, H.A. Gasteiger, Handbook of Fuel Cells – Fundamentals, Technology and Applications, in, vol. 3, John Wiley & Sons, Chichester, 2003.
[2] J. Garche, C.K. Dyer, P.T. Moseley, Z. Ogumi, D.A.J. Rand, B. Scrosati, Encyclopedia of Electrochemical Power Sources, in, vol. 3, Elsevier, Amsterdam, 2009, pp. 4538.
[3] L. Carrette, K.A. Friedrich, U. Stimming, Fuel Cells 1 (2001) 5-39.
[4] C.-Y. Wang, Chemical Reviews 104 (2004) 4727-4766.
[5] R.J. Bellows, M.Y. Lin, M. Arif, A.K. Thompson, D. Jacobson, Journal of The Electrochemical Society 146 (1999) 1099-1103.
[6] R. Satija, D.L. Jacobson, M. Arif, S.A. Werner, Journal of Power Sources 129 (2004) 238-245.
[7] N. Pekula, K. Heller, P. Chuang, A. Turhan, M. Mench, J. Brenizer, K. Unlu, Nuclear Instruments and Methods in Physics Research Section A: Accelerators, Spectrometers, Detectors and Associated Equipment 542 (2005) 134-141.
[8] D. Kramer, J. Zhang, R. Shimoi, E. Lehmann, A. Wokaun, K. Shinohara, G.G. Scherer, Electrochimica Acta 50 (2005) 2603-2614.
[9] P. Boillat, D. Kramer, B.C. Seyfang, G. Frei, E. Lehmann, G.G. Scherer, A. Wokaun, Y. Ichikawa, Y. Tasaki, K. Shinohara, Electrochemistry Communications 10 (2008) 546-550.
[10] C. Hartnig, I. Manke, N. Kardjilov, A. Hilger, M. Grünerbel, J. Kaczerowski, J. Banhart, W. Lehnert, Journal of Power Sources 176 (2008) 452-459.
[11] A. Schröder, K. Wippermann, J. Mergel, W. Lehnert, D. Stolten, T. Sanders, T. Baumhöfer, D.U. Sauer, I. Manke, N. Kardjilov, A. Hilger, J. Schloesser, J. Banhart, C. Hartnig, Electrochemistry Communications 11 (2009) 1606-1609.
[12] A. Schröder, K. Wippermann, W. Lehnert, D. Stolten, T. Sanders, T. Baumhöfer, N. Kardjilov, A. Hilger, J. Banhart, I. Manke, Journal of Power Sources 195 (2010) 4765-4771.
[13] I. Manke, C. Hartnig, M. Grunerbel, W. Lehnert, N. Kardjilov, A. Haibel, A. Hilger, J. Banhart, H. Riesemeier, Applied Physics Letters 90 (2007) 174105.
[14] C. Hartnig, I. Manke, R. Kuhn, N. Kardjilov, J. Banhart, W. Lehnert, Applied Physics Letters 92 (2008) 134106.
[15] I. Manke, C. Hartnig, N. Kardjilov, H. Riesemeier, J. Goebbels, R. Kuhn, P. Krüger, J. Banhart, Fuel Cells 10 (2010) 26-34.
[16] C. Hartnig, I. Manke, J. Schloesser, P. Krüger, R. Kuhn, H. Riesemeier, K. Wippermann, J. Banhart, Electrochemistry Communications 11 (2009) 1559-1562.
[17] R. Thiedmann, C. Hartnig, I. Manke, V. Schmidt, W. Lehnert, Journal of the Electrochemical Society 156 (2009) B1339-B1347.

[18] J. Banhart, A. Borbely, K. Dzieciol, F. Garcia-Moreno, I. Manke, N. Kardjilov, A.R. Kaysser-Pyzalla, M. Strobl, W. Treimer, International Journal of Materials Research 101 (2010) 1069-1079.

[19] M. Capellas, ESRFnews 52 (2009) 12-13.

[20] W. Görner, M.P. Hentschel, B.R. Müller, H. Riesemeier, M. Krumrey, G. Ulm, W. Diete, U. Klein, R. Frahm, Nuclear Instruments and Methods in Physics Research Section A: Accelerators, Spectrometers, Detectors and Associated Equipment 467-468 (2001) 703-706.

[21] P. Zhou, C.W. Wu, Journal of Power Sources 195 (2010) 1408-1415.

[22] Z. Lu, M.M. Daino, C. Rath, S.G. Kandlikar, International Journal of Hydrogen Energy 35 (2010) 4222-4233.

[23] D. Gerteisen, T. Heilmann, C. Ziegler, Journal of Power Sources 177 (2008) 348-354.

[24] R. Alink, D. Gerteisen, W. Mérida, Fuel Cells DOI: 10.1002/fuce.201000110 (2011) article in press.
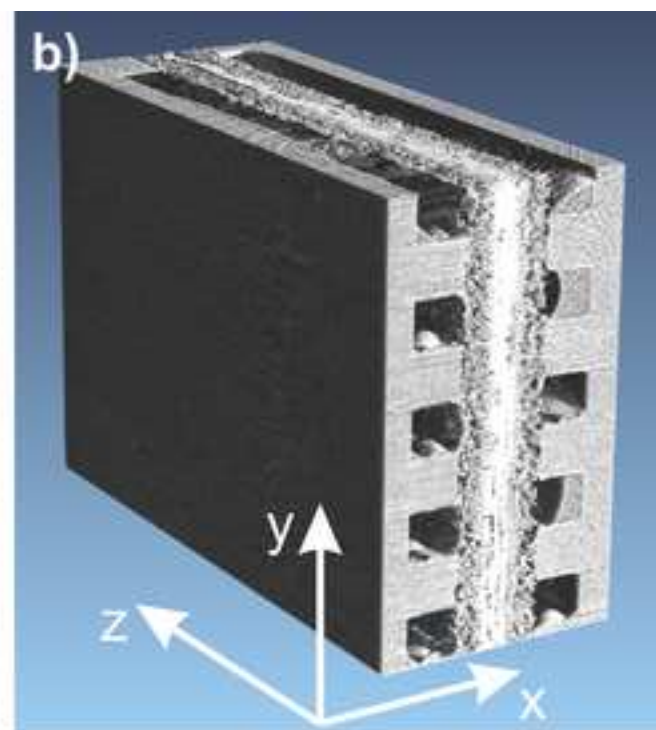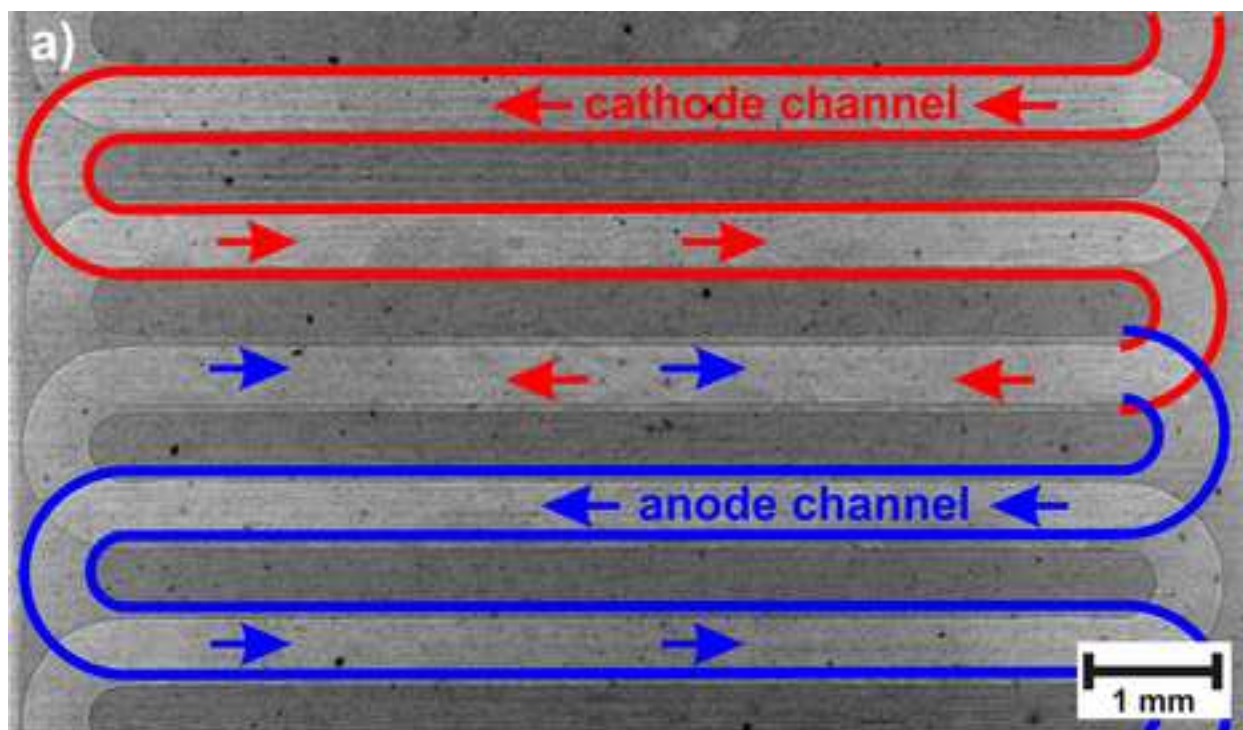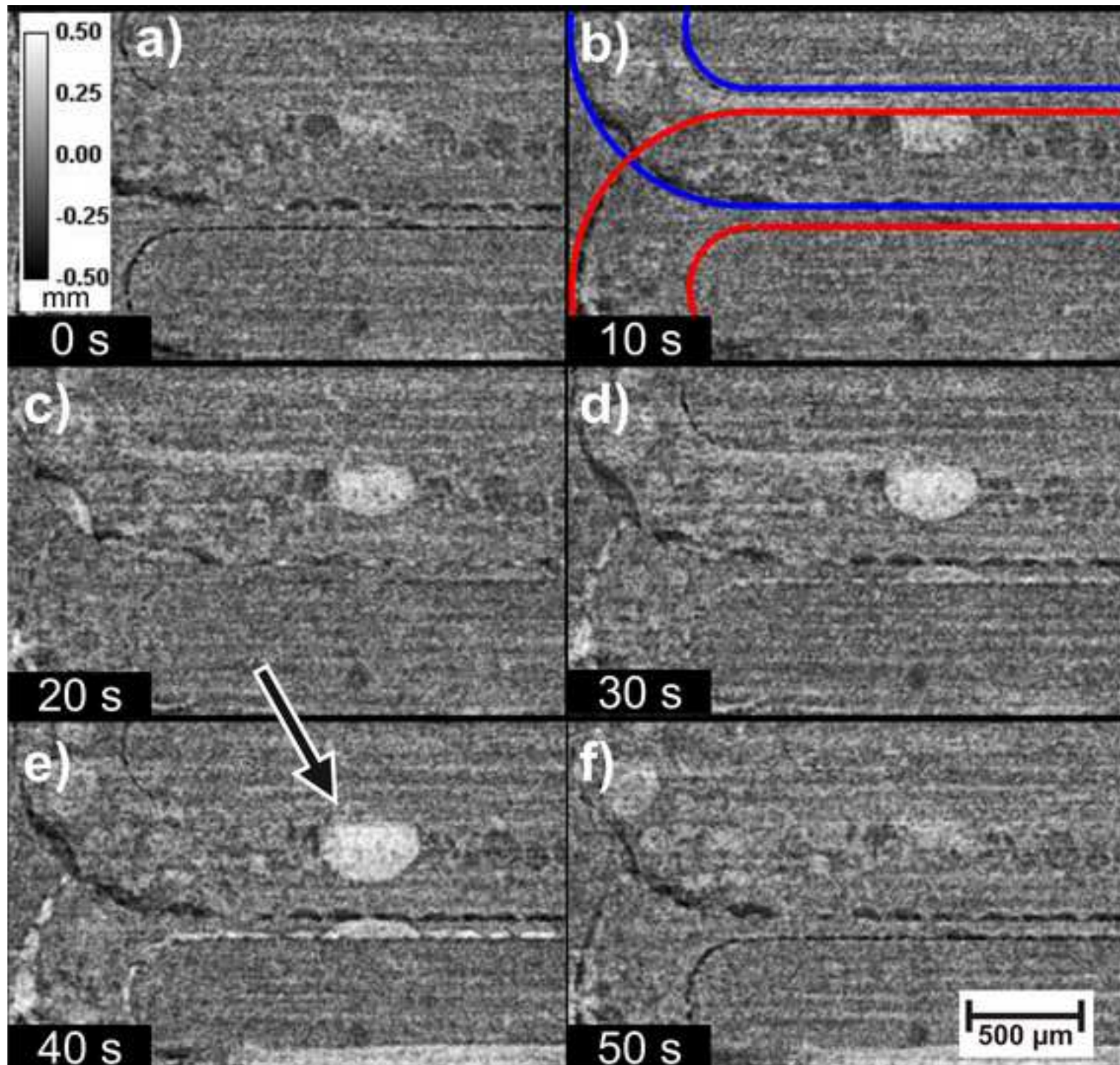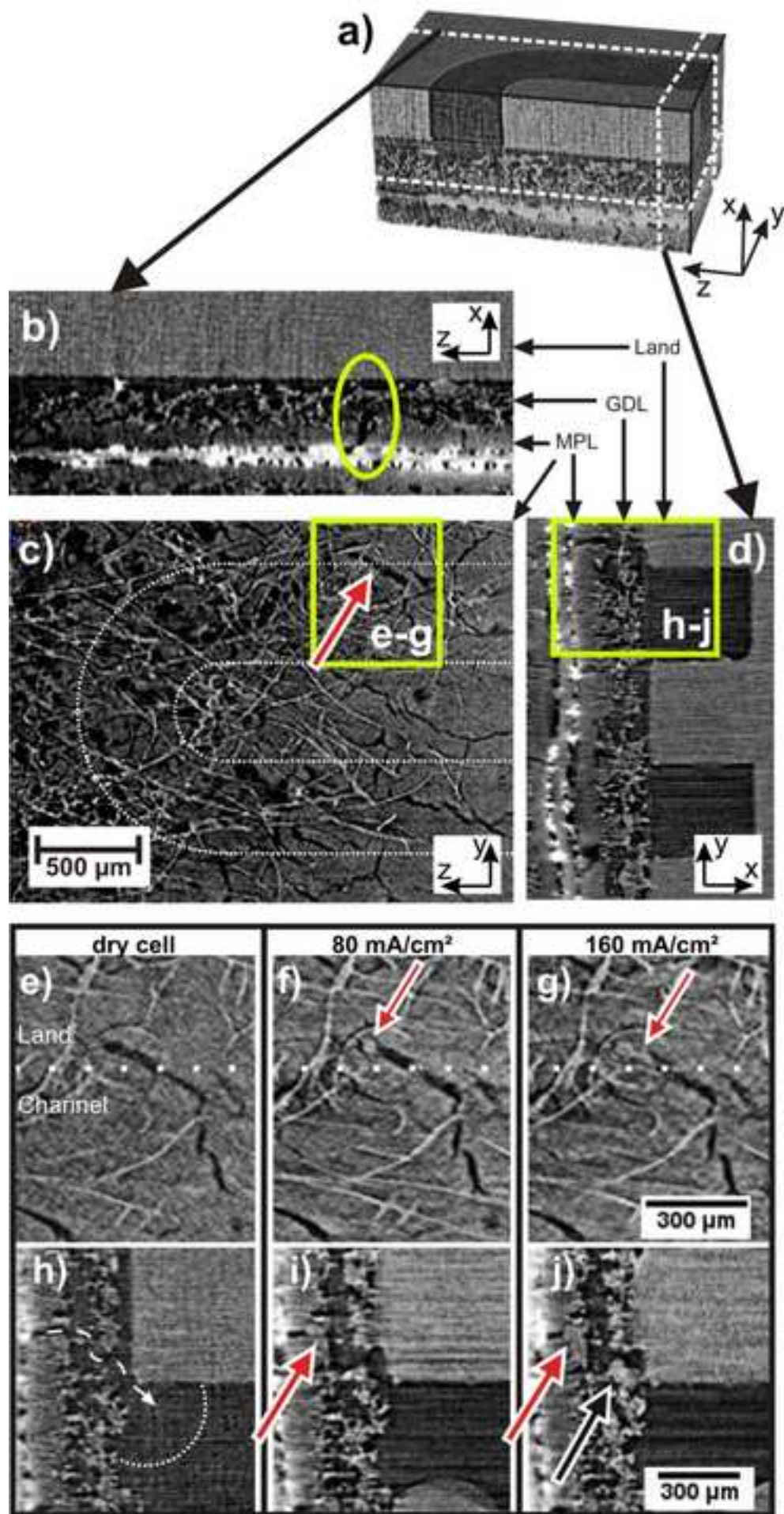
d. Figure Captions

Figure 1:

a: Radiograph with marked channels of the anode and cathode including gas flow direction.

b: Cutout of the reconstructed 3D structure of the cell.

Figure 2

a-f: Series of radiographs taken during cell operation at 160 mA/cm² current density. A droplet (marked by an arrow) in the cathode channel (highlighted in red) evolves during 45 seconds to about 20 nl volume.

Figure 3:

a: Cutout of a tomogram

b-d: Slices of the tomogram in different orientations at the position of the growing droplet seen in figure 2. A crack in the MPL (red arrow in c) and a GDL pore align to build up a transport path (d).

e-j: Comparison of the regions boxed in yellow in c) and d) as observed in the dry cell and at 80 and 160 mA/cm².